Effects of water phase change on the material response of low-density carbon-phenolic ablators

Ali D. Omidy[1] and Francesco Panerai[2]
University of Kentucky, Lexington, KY 40506

Jean R. Lachaud[3]
University of California Santa Cruz, Moffett Field, CA 94043

Nagi N. Mansour[4]
NASA Ames Research Center, Moffett Field, CA 94043

Alexandre Martin[5]
University of Kentucky, Lexington, KY, USA 40506

[1] Research Assistant, Department of Mechanical Engineering; ali.omidy2@uky.edu
[2] Post Doctoral Research Associate, Department of Mechanical Engineering; francesco.panerai@uky.edu
[3] Scientist, Silicon Valley Initiative. Senior Member AIAA; jlachaud@ucsc.edu
[4] Chief Scientist for Modeling and Simulation, TN Division. Associate Fellow AIAA; nagi.n.mansour@nasa.gov
[5] Assistant Professor, Department of Mechanical Engineering. Associate Fellow AIAA; alexandre.martin@uky.edu

I. Introduction

During atmospheric entry, the shock layer in front of spacecraft converts kinetic energy into heat. In order to protect the vehicle from this extreme heat, thermal protection systems (TPS) are used. One option for TPS material is a low-density ablator, made of a porous carbon fiber preform impregnated with a phenolic resin. Through various complex mechanisms, this class of material uses the incoming heat to trigger chemical reactions that will reduce the surface heat flux [1] as well as decrease its conversion into thermal energy [2, 3]. The Phenolic Impregnated Carbon Ablator (PICA) [4] developed by NASA belongs to this class of materials. PICA was successfully used on various entry vehicles such as the *Stardust Sample Return Capsule* [5], SpaceX's *Dragon* spacecraft (using a variant branded PICA-X) [6] and, more recently, the *Mars Science Laboratory* (MSL) entry spacecraft [7].

II. Mars Science Lab entry data

The atmospheric entry of the MSL spacecraft was of great importance to the scientific community, as the heat shield was equipped with the *MSL Entry, Descent, and Landing Instrumentation* (MEDLI) suite [8]. MEDLI was composed of seven surface pressure ports, known as *Mars Entry Atmospheric Data System* (MEADS), as well as a combination of seven sets of thermocouples (TC) and a *Hollow aErothermal Ablation and Temperature* (HEAT) sensor [9], known as the *MEDLI Integrated Sensor Plug* (MISP). Each set of MISP used four TCs to measure temperature at specific depths within the heat shield, as well as the HEAT sensor to measure the propagation of an isotherm. The location of the MEADS and MISP sensors on the surface of MSL is shown in Figs. 1(a) and 1(b), respectively.

As documented in the literature [8, 10–14], the MISP data showed significant differences when compared with the predictive solutions of FIAT, the one-dimensional material response (MR) code used for the design of heat shields [15]. Post-flight simulations performed using the MEDLI near-surface TC as a boundary condition (the so-called "TC driver method") produced better results [11]. These results suggest that variabilities in the atmospheric conditions and the simplifications used in the aerothermal boundary conditions are mostly responsible for the discrepancies [10]. Moreover, uncertainty and

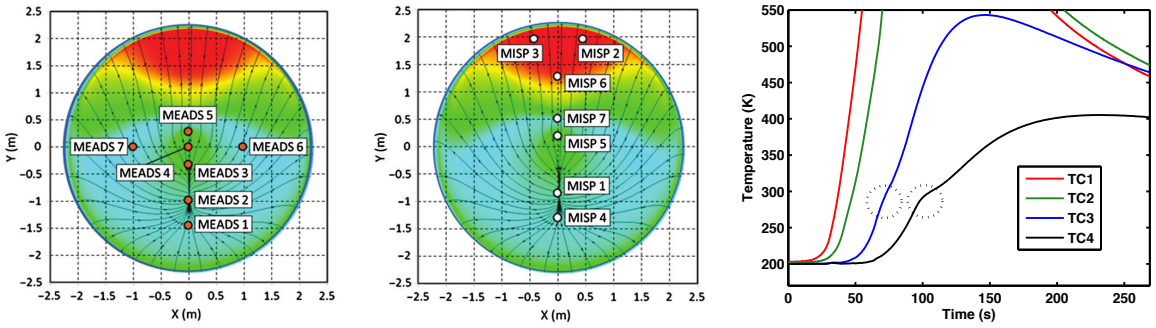

(a) Location of the MEADS sensors that measure the pressure at the surface of the heat shield – the color contours illustrate heating (image from Bose et al. [10], with permission)

(b) Location of the MISP sensors that measure the temperature within the heat shield – the color contours illustrate heating (image from Bose et al. [10], with permission)

(c) Temperature histories obtained by MISP 2, with the "hump" visible on TC3 and TC4 (image from Mahzari et al. [11], with permission)

Fig. 1: Instrumentation of the heat shield of the Mars Science Laboratory entry spacecraft

sensitivity analysis demonstrated that varying the values of the material properties based on known uncertainties, as well as accounting for experimental errors resulted in better general agreements with the flight data [11]. However, all of these studies still failed to model a specific temperature behavior observed in the data taken by the two deepest TCs. For these measurements, the temperature deviates from the expected smooth rise, forming a "hump" near 300 K. The phenomenon is shown in Fig. 1(c) for the MISP2 sensor, highlighted by a dashed circle. It is important to point out that it was also observed in most of the arc-jet tests performed on the MISP plugs, flight thermocouple data from the Mars Pathfinder entry (SLA-561V heat-shield), as well as in other arc-jet tested materials such as AVCOAT.[16–18]

Since attempts at modeling the hump by modifying the thermal properties were unsuccessful in reproducing the phenomenon [8, 10–14], it is reasonable to assume a shortcoming of the current model at temperatures below 400 K. The present analysis provides a plausible pathway of investigation to fulfill the scientific interest in understanding the nature of this phenomenon. Moreover, since the

hump occurs in the region near the back face of the heat shield, at the interface with the substructure (the "bond line"), a proper modeling and understanding of the hump might also reveal whether the phenomenon needs to be considered in future TPS design.

III. Effect of water on the material properties of PICA

The thermal response of porous carbon/phenolic ablators, more specifically the heat transfer, can be significantly altered by the water content of the material. The presence of water could be due to (i) residual atmospheric moisture, or (ii) formation of H_2O as a result of the decomposition of phenolic resin. The effects of the water content on the material properties of the ablator is not accounted for in traditional MR models.

Process (i) assumes that water vapor from the atmosphere is absorbed by the material while the TPS is going through the manufacturing and assembly stages, or waiting on the launch pad in moisture heavy Florida [19]. Since the heat shield of MSL was coated with a thin layer of low-outgassing silicon to prevent contamination [20], moisture might be adsorbed in the porous material as the vehicle travels to its destination. Even without the coating, the moisture could remain trapped within the porous material and then solidify due to flash freezing when exposed to the vacuum of outer space.

Evidence of the presence of water due to process (ii) has been observed during experimental analysis of gaseous products resulting from phenolic decomposition [21–24]. The first species produced by the decomposition is H_2O, appearing in significant quantity around 325 K, reaching a maximum concentration around 675 K, and essentially vanishing after 950 K. Molecular dynamics simulations also showed that H_2O is formed through the pyrolysis of phenolic resin [25, 26]. Because the pyrolysis gases are transported through the porous structure [27–31], part of the water vapor created in the pyrolysis zone travels toward the back of the ablator [30]. In this region, the temperature is much lower, and the moisture condenses. Once the vapor has condensed, the liquid droplets remain trapped within the pores and do not travel to colder regions of the material, where they would freeze.

It is reasonable to assume that process (i) is at-least partly accounted for in the thermogravimetric

analysis (TGA) used to produce the PICA decomposition model [32]. However, process (ii) is not considered since it is due to the transient and multi-dimensional nature of the temperature and pressure distribution within the ablator. For this reason, the present investigative analysis focuses on process (ii).

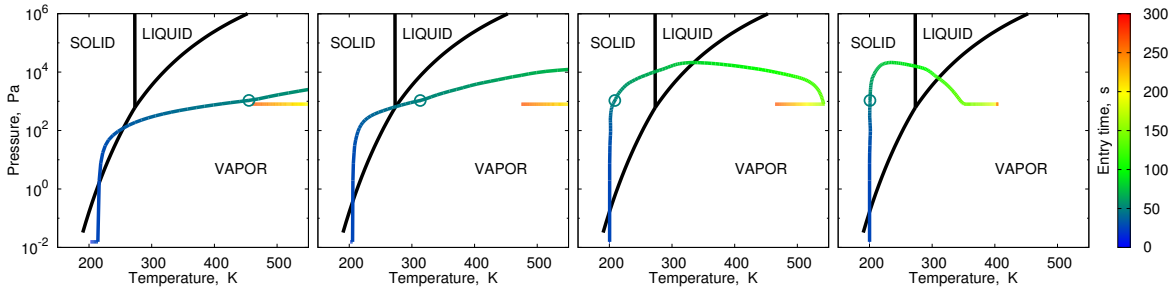

(a) TC1 depth = 0.106 in (b) TC2 depth = 0.203 in (c) TC3 depth = 0.456 in (d) TC4 depth = 0.700 in

Fig. 2: Phase change of water as a function of temperature, pressure, and time at the location for the four thermocouples of MISP 2. The time at which pyrolysis reaction at the surface are significant is indicated on each graph by the symbol ⊙.

During the entry phase, as the spacecraft travels through the upper atmosphere, the local temperature and pressure vary throughout the TPS. Figure 2 illustrates this variation for the four TCs of the second MISP. This MISP is chosen because it was located in the region of maximum heat flux, as shown in Fig. 1(b). The local phase of water is obtained by superimposing the phase diagram of water on the time-dependent local thermodynamic state. The pressure used to generate the graph is the surface pressure predicted by a flow field simulation using reconstructed data from MEADS [10, 33, 34].

The symbol ⊙ on each panel of Fig. 2 indicates the local thermodynamic state of H_2O at each TC location, when the surface reaches 600 K. This temperature, occurring approximately at 50 s, promotes significant pyrolysis decomposition. Although minor decomposition is seen between 400 and 600 K, mass loss is negligible in this range [21–24, 35]. As shown in Fig. 2(a) and 2(b), after 50 s, any H_2O

being transported to the region between TC1 and TC2 would remain in vapor phase. However, H_2O reaching the location of TC3 and TC4 would condense in liquid phase. The occurrence of the hump, observed for TC3 and TC4 but not for TC1 and TC2, is speculated to be caused by the condensation of H_2O generated by the pyrolysis gas being transported within the ablator.

To evaluate the effect of water condensation, an investigative model that modifies the local thermal conductivity of PICA based on the presence of water is implemented in the material response code PATO [36]. PATO is a fully portable library for OpenFOAM[6], an open-source finite-volume computational fluid dynamics (CFD) software released by OpenCFD Limited. The PATO library is specifically implemented to test innovative physics-based models for reactive porous materials subjected to high-temperature environments. In the present analysis, the state-of-the-art ablation models used for design [37] are used in PATO. When using these models, PATO reproduces accurately the results of FIAT [38].

The investigative model used here, which could be used in most material response codes, modifies the local thermal conductivity k of the whole material according to the presence of water, as well as its phase. This is achieved using the *parallel conductivity model* [39], which simply adds a term to the conductivity of PICA:

$$k = k_{\mathrm{PICA}} + \psi k_{\mathrm{H_2O}} \tag{1}$$

The value used for k_{PICA} is taken from Mahzari et al. [11]. The value of the conductivity of water $k_{\mathrm{H_2O}}$ depends on its phase, and is determined using the local temperature and pressure inside the ablator, as illustrated in the phase diagram shown in Fig. 2:

$$k_{\mathrm{H_2O}} = \begin{cases} 0.0 & \text{if in gas phase} \\ k_{\mathrm{H_2O}_{(l)}} & \text{if in liquid phase} \end{cases} \tag{2}$$

[6] The PATO library is not endorsed by OpenCFD Limited, the producer of the OpenFOAM software and owner of the OPENFOAM® and OpenCFD® trademarks. www.openfoam.org/ [retrieved 11 November 2014].

The value of $k_{\mathrm{H_2O}_{(l)}}$ depends on the local temperature and pressure [40, p. 6-1]. As previously mentioned, the model assumes that the water vapor condenses to liquid form before reaching the regions where it could turn to ice, which is why the solid phase is not considered in Eq. 2. It is to be noted that the presence of ice would increase the overall conductivity of the material even more.

The parameter ψ can be seen as representing the fraction of water in the system. Because water is assumed to appear only through the pyrolysis process, this added conductivity is applied when the estimated surface temperature of the MISP reaches the temperature that promotes significant pyrolysis reactions, approximated at 50 s. Therefore, ψ is specified according to the following:

$$\psi = \begin{cases} 0.0 \ \forall \ t \ \in \ [0, 50[\text{ s} \\ \\ \psi_w \ \forall \ t \ \in \ [50, 268] \text{ s} \end{cases} \tag{3}$$

Figure 3 presents the results for the four thermocouples of MISP 2 for a simulation using the investigative model, using a value of $\psi_w = 0.3$. For these results, the TC driver boundary condition is used at the surface. As for the backface, an adiabatic boundary condition is applied. Due to the unavailability of material properties, the substructure below the heat shield material is not modeled. Other studies [8, 11, 12] performed this modeling, and showed a better agreement at the end of the trajectory, especially for the two deepest thermocouples.

As seen in the figure, the hump appears in the two deepest thermocouple measurements. The model was tested on all other MISP, and produced similar results (see Fig. A1 of the *Supplemental Material*). Various values of ψ_w were also tested, ranging from 0 (no water) to 0.80 (pores filled with water). It was observed that the size of the hump was directly proportional to the amount of water (see Fig. A2 of the *Supplemental Material*). Other parameters, such as heat capacity c_p and enthalpy of formation Δh_f^0, were also tested using a similar approach, and produced similar behavior.

The value of ψ_w should not be regarded as an evaluation of the amount of water present in the TPS. This could only be achieved once a physical model is used. The present results simply point out that the hump appears if the thermal properties are modified according to the water content.

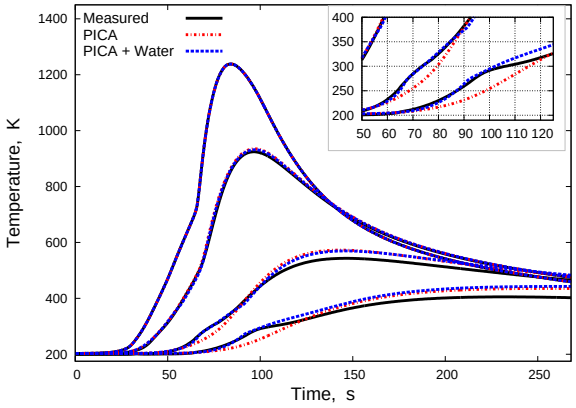

Fig. 3: Thermocouple readings for MISP 2 using a modified thermal conductivity model accounting for the presence of water. The new results are compared to the previous results obtained using the estimated PICA conductivity from Mahzari et al. [11], as well as the MISP flight data.

IV. Outlook

The hypotheses stating that the presence of water within the heat shield material may affect the material properties, and hence, the heating rates, is worth exploring further. Using a simple investigative model that modifies locally the thermal conductivity of the material according to the phases of water, a temperature hump that closely resembles the one observed in the flight data was generated. These preliminary results are encouraging and motivate the addition of a condensed water phase in a physics-based model for ablative materials. More than just conductivity, the new model will need to track other volume-averaged material properties that could be affected by the presence of liquid water, such as density, heat capacity, porosity, and enthalpy of formation.

To fully verify the hypothesis, experimental studies will also be needed to determine the quantity of water content of PICA. Once it has been quantified, a more accurate assessment of the modification to the material properties may be performed.

ACKNOWLEDGMENTS

Financial support for this work was provided in part by NASA Kentucky EPSCoR Award NNX13AN04A, NASA Kentucky Space Grant Award NNX10AL96H, NASA Award NNX14AC93A, and NASA Award NNX14AI97G. Part of this work was also performed under the Entry System Modeling Project (M.J. Wright project manager) of the NASA Game Changing Development (GCD) Program. A.D. Omidy is thankful to D.B. Hash and the summer program at NASA Ames Research Center, as well as M. Mahzari, A.J. Amar, and T.R. White for the numerous insightful discussions. Finally, the authors are grateful to S.C.C. Bailey, K.A. Tagavi, M.J. Wright, A.J. Vanaerschot, B.A. Biegel and D.B. Hash for carefully reviewing the manuscript.

Supplementary material associated with this article can be found, in the online version at http://dx.doi.org/xxxxxxxxxxxx.

REFERENCES

[1] Martin, A. and Boyd, I. D., "Modeling of heat transfer attenuation by ablative gases during the Stardust re-entry," *Journal of Thermophysics and Heat Transfer*, Vol. 29, No. 3, 2015.
doi:10.2514/1.T4202

[2] Amar, A. J., Blackwell, B. F., and Edwards, J. R., "One-Dimensional Ablation Using a Full Newton's Method and Finite Control Volume Procedure," *Journal of Thermophysics and Heat Transfer*, Vol. 22, No. 1, 2008, pp. 72–82.
doi:10.2514/1.29610

[3] Amar, A. J., Blackwell, B. F., and Edwards, J. R., "Development and Verification of a One-Dimensional Ablation Code Including Pyrolysis Gas Flow," *Journal of Thermophysics and Heat Transfer*, Vol. 23, No. 1, 2009, pp. 59–71.
doi:10.2514/1.36882

[4] Tran, H. K., Johnson, C. E., Rasky, D. J., Hui, F. C. L., Hsu, M.-T., and Chen, Y. K., "Phenolic Impregnated Carbon Ablators (PICA) for Discovery class missions," AIAA Paper 1996-1911, 1996.
doi:10.2514/6.1996-1911

[5] Kontinos, D. A. and Wright, M. J., "Introduction: Atmospheric Entry of the Stardust Sample Return Capsule," *Journal of Spacecraft and Rockets*, Vol. 47, No. 5, 2010, pp. 705–707.
doi:10.2514/1.51522

[6] "SpaceX manufactured heat shield material passes high temperature tests simulating [Press release]," Retreived on November 12, 2014 from http://www.spacex.com/press/2012/12/19/spacex-manufactured-heat-shield-material-passes-high-temperature-tests-simulating, February 23 2009.

[7] "Seeing red," *Nature*, Vol. 479, No. 7374, 2011, pp. 446–446.
doi:10.1038/479446a

[8] Bose, D., Santos, J. A., Rodriguez, E., White, T. R., and Mahzari, M., "Mars Science Laboratory Heat Shield Instrumentation and Arc Jet Characterization," AIAA Paper 2013-2778, 2013.
doi:10.2514/6.2013-2778

[9] Santos, J. A., Oishi, T., and Martinez, E. R., "Isotherm Sensor Calibration Program for Mars Science Laboratory Heat Shield Flight Data Analysis," AIAA Paper 2011-3955, 2011.
doi:10.2514/6.2011-3955

[10] Bose, D., White, T., Mahzari, M., and Edquist, K., "Reconstruction of Aerothermal Environment and Heat Shield Response of Mars Science Laboratory," *Journal of Spacecraft and Rockets*, Vol. 51, No. 4, 2014, pp. 1174–1184.
doi:10.2514/1.A32783

[11] Mahzari, M., Braun, R. D., White, T. R., and Bose, D., "Inverse Estimation of the Mars Science Laboratory Entry Aeroheating and Heatshield Response," *Journal of Spacecraft and Rockets*, 2015.
doi:10.2514/1.A33053

[12] White, T. R., Mahzari, M., Bose, D., and Santos, J. A., "Post-flight Analysis of the Mars Science Laboratory Entry Aerothermal Environment and Thermal Protection System Response," AIAA Paper 2013-2779, 2013.
doi:10.2514/6.2013-2779

[13] Bose, D., Olson, M., Laub, B., White, T. R., Feldman, J., Santos, J., and Mahzari, M., "Initial Assessment of Mars Science Laboratory Heatshield Instrumentation and Flight Data," AIAA Paper 2013-908, 2013.
doi:10.2514/6.2013-908

[14] Mahzari, M., Braun, R. D., White, T. R., and Bose, D., "Preliminary Analysis of the Mars Science Laboratory's Entry Aerothermodynamic Environment and Thermal Protection System Performance," AIAA Paper 2013-0185, 2013.
doi:10.2514/6.2013-185

[15] Chen, Y.-K. and Milos, F. S., "Ablation and Thermal Response Program for Spacecraft Heatshield Anal-

ysis," *Journal of Spacecraft and Rockets*, Vol. 36, No. 3, 1999, pp. 475–483.
doi:10.2514/2.3469

[16] Smith, D. L., Omidy, A. D., Weng, H., White, T. R., and Martin, A., "Effects of Water Presence on Low Temperature Phenomenon in PICA," AIAA Paper 2015-2505, 2015.
doi:10.2514/6.2015-2505

[17] Smith, D. L., White, T. R., and Martin, A., "Comparisons of PICA In-depth Material Performance and Ablator Response Modeling from MEDLI Arc Jet Tests," AIAA Paper 2015-2664, 2015.
doi:10.2514/6.2015-2664

[18] Kobayashi, Y., Sakai, T., Suzuki, T., Fujita, K., Okuyama, K., Kato, S., and Kitagawa, K., "An Experimental Study on Thermal Response of Low Density Carbon-Phenolic Ablators," AIAA Paper 2009-1587, 2009.
doi:10.2514/6.2009-1587

[19] Sepka, S., Gasch, M., Beck, R. A., and White, S., "Testing of Candidate Rigid Heat Shield Materials at LHMEL for the Entry, Descent, and Landing Technology Development Project," *Advanced Ceramic Coatings and Materials for Extreme Environments II: Ceramic Engineering and Science Proceeding*, Vol. 33, 2012, pp. 129–156.
doi:10.1002/9781118217474.ch11

[20] Szalai, C., Slimko, E., and Hoffman, P., "Mars Science Laboratory Heatshield Development, Implementation, and Lessons Learned," *Journal of Spacecraft and Rockets*, Vol. 51, No. 4, 2014, pp. 1167–1173.
doi:10.2514/1.A32673

[21] Wong, H.-W., Peck, J., Edwards, R., Reinisch, G., Lachaud, J., and Mansour, N. N., "Measurement of pyrolysis products from phenolic polymer thermal decomposition," AIAA Paper 2014-1388, 2014.
doi:10.2514/6.2014-1388

[22] Wong, H.-W., Peck, J., Assif, J., Lachaud, J., and Mansour, N. N., "Quantitative determination of species production from the pyrolysis of the Phenolic Impregnated Carbon Ablator (PICA)," AIAA Paper 2015-1447, 2015.
doi:10.2514/6.2015-1447

[23] Wong, H.-W., Peck, J., Bonomi, R. E., Assif, J., Panerai, F., Reinisch, G., Lachaud, J., and Mansour, N. N., "Quantitative determination of species production from phenol-formaldehyde resin pyrolysis," *Polymer Degradation and Stability*, January 2015, pp. 122–131.

doi:10.1016/j.polymdegradstab.2014.12.020

[24] Bessire, B. K., Lahankar, S. A., and Minton, T. K., "Pyrolysis of Phenolic Impregnated Carbon Ablator (PICA)," *ACS Appl. Mater. Interfaces*, Vol. 7, No. 3, 2015, pp. 1383–1395.
doi:10.1021/am507816f

[25] Qi, T., Bauschlicher, Jr., C. W., Lawson, J. W., Desai, T. G., and Reed, E. J., "Comparison of ReaxFF, DFTB, and DFT for Phenolic Pyrolysis. 1. Molecular Dynamics Simulations," *J. Phys. Chem. A*, Vol. 117, 2013, pp. 11115–11125.
doi:10.1021/jp4081096

[26] Bauschlicher, Jr., C. W., Qi, T., Reed, E. J., Lawson, J. W., and Desai, T. G., "Comparison of ReaxFF, DFTB, and DFT for Phenolic Pyrolysis. 2. Elementary Reaction Paths," *J. Phys. Chem. A*, Vol. 117, 2013, pp. 11126–11135.
doi:10.1021/jp408113w

[27] Martin, A. and Boyd, I. D., "Non-Darcian behavior of pyrolysis gas in a thermal protection system," *Journal of Thermophysics and Heat Transfer*, Vol. 24, No. 1, 2010, pp. 60–68.
doi:10.2514/1.44103

[28] Weng, H., Bailey, S. C. C., and Martin, A., "Numerical study of iso-Q sample geometric effects on charring ablative materials," *International Journal of Heat and Mass Transfer*, Vol. 80, January 2015, pp. 570–596.
doi:10.1016/j.ijheatmasstransfer.2014.09.040

[29] Weng, H. and Martin, A., "Numerical Investigation of Thermal Response Using Orthotropic Charring Ablative Material," *Journal of Thermophysics and Heat Transfer*, Vol. 29, No. 3, 2015.
doi:10.2514/1.T4576

[30] Weng, H. and Martin, A., "Numerical Investigation on Charring Ablator Geometric Effects: Study of Stardust Sample Return Capsule Heat Shield," AIAA Paper 2015-0211, 2015.
doi:10.2514/6.2015-0211

[31] Weng, H. and Martin, A., "Multidimensional modeling of pyrolysis gas transport inside charring ablative materials," *Journal of Thermophysics and Heat Transfer*, Vol. 28, No. 4, 2014, pp. 583–597.
doi:10.2514/1.T4434

[32] Milos, F. and Chen, Y.-K., "Ablation and Thermal Property Model for Phenolic Impregnated Carbon Ablator (PICA)," Technical Memorandum 2009-215377, NASA Ames Research Center, Moffett Field, CA, March 2009.

[33] Karlgaard, C. D., Kutty, P., Schoenenberger, M., Shidner, J., and Munk, M., "Mars Entry Atmospheric Data System Trajectory Reconstruction Algorithms and Flight Results," AIAA Paper 2013-0028, 2013. doi:10.2514/6.2013-28

[34] Edquist, K. T., Hollis, B. R., Johnston, C. O., Bose, D., White, T. R., and Mahzari, M., "Mars Science Laboratory Heatshield Aerothermodynamics: Design and Reconstruction," AIAA Paper 2013-2781, 2013. doi:10.2514/6.2013-2781

[35] Martin, A., Cozmuta, I., Boyd, I. D., and Wright, M. J., "Kinetic rates for gas phase chemistry of phenolic based carbon ablator decomposition in atmospheric air," *Journal of Thermophysics and Heat Transfer*, Vol. 29, No. 2, 2015, pp. 222–240. doi:10.2514/1.T4184

[36] Lachaud, J. and Mansour, N. N., "Porous-Material Analysis Toolbox Based on OpenFOAM and Applications," *Journal of Thermophysics and Heat Transfer*, Vol. 28, No. 2, 2014, pp. 191–202. doi:10.2514/1.T4262

[37] Lachaud, J., Magin, T. E., Cozmuta, I., and Mansour, N. N., "A short review of ablative-material response models and simulation tools," *7th European Symposium on Aerothermodynamics*, 2011, pp. 1–9.

[38] Omidy, A. D., Panerai, F., Lachaud, J., Mansour, N., Cozmuta, I., and Martin, A., "Code-to-Code Comparison, and Material Response Modeling of Stardust and MSL using PATO and FIAT," Contractor report, NASA Ames Research Center, Moffett Field, CA, 2015, In preparation.

[39] Kandula, M., "On the Effective Thermal Conducivity of Porous Packed Beds with Uniform Spherical Particles," *Journal of Porous Media*, Vol. 14, No. 10, 2011, pp. 919–926. doi:10.1615/JPorMedia.v14.i10.70

[40] Haynes, W. M., editor, *CRC Handbook of Chemistry and Physics*, 95th ed., CRC Press, 2014.

APPENDIX A. SUPPLEMENTARY MATERIAL

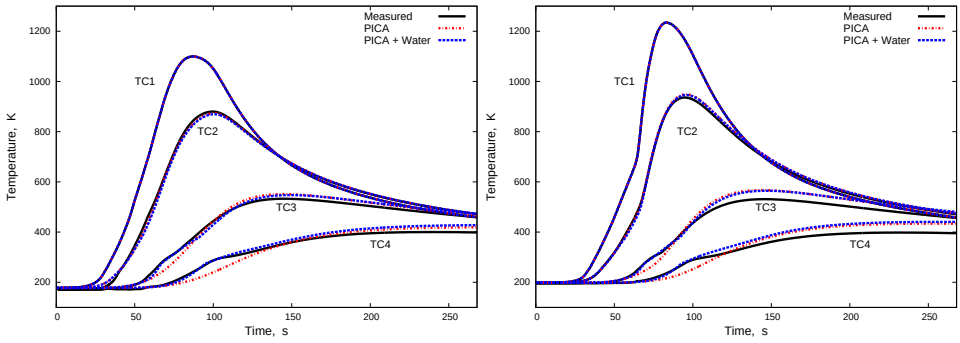

(a) MISP 1

(b) MISP 3

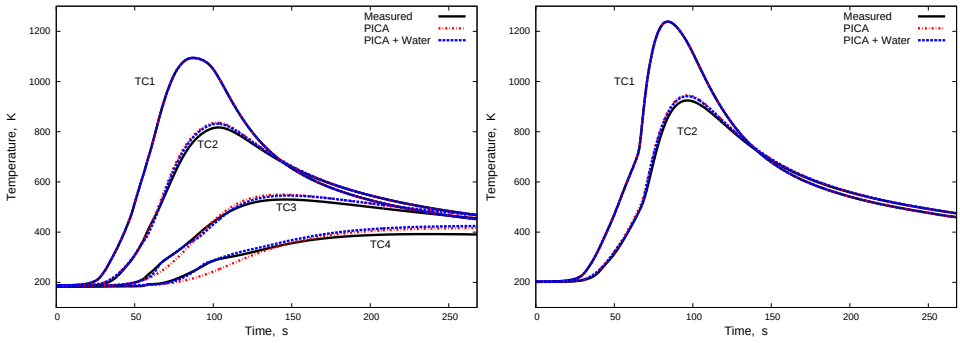

(c) MISP 4

(d) MISP 5

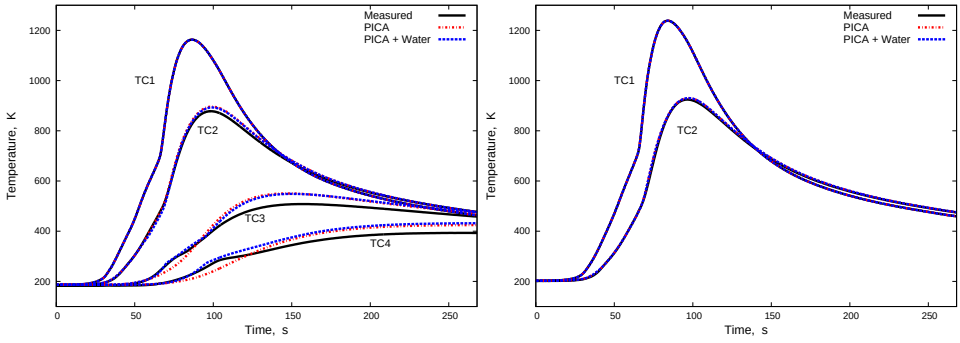

(e) MISP 6

(f) MISP 7

Fig. A1: Comparison of the investigative model, the baseline estimated model (from Mahzari et al. [11]), and the measured flight data for all MEDLI Integrated Sensor Plug (MISP) of Mars Science Laboratory (MSL), except MISP 2, which is discussed in the main text

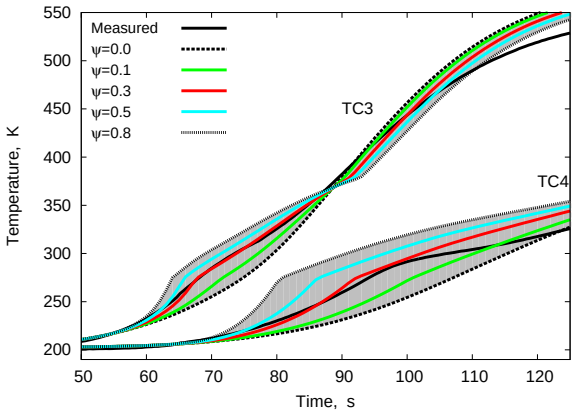

Fig. A2: Comparison of the measured flight data for MISP2 and the investigative model applied to k, using a volume fraction of water ψ_w ranging from 0 to 0.8